A Coin Detection System by Coupled Printed Spiral Inductors

Junichi Fukatani*, Sho Yamaguchi*, Masayuki Yamauchi†, Kazuhisa Yoshimatsu†, Hisashi Aomori* and Mamoru Tanaka*
*Department of Electrical and Electronics Engineering, Sophia University
7-1 Kioi, Chiyoda-ku, Tokyo, 102-8554, JAPAN
†Department of Electronics and Computer Engineering, Hiroshima Institute of Technology University
2-1-1 Miwake, Saeki-ku, Hiroshima-shi, Hiroshima, 731-5193, JAPAN
J.Fukata@gmail.com, yamagus8@yahoo.co.jp, yamauchi@ieee.org,
yoshimatsu.k@gmail.com, aomori@ieee.org, Mamoru.Tanaka@gmail.com

Abstract: This paper describes a coin detection system using coupled Printed Spiral Inductors (PS-Inductors). In this research, the PS-Inductor is composed of copper foil spiral on the printed board. As an advantages, the PS-Inductor can be made easily and does not need the iron core. The experimental measurement and the theoretical calculation of the inductance of the PS-Inductor are derived. This enables the easily realizable coin detection system using PS-Inductor. In this system, a coin can be identified as changes of the mutual inductance of coupled PS-Inductors. The mutual inductance is investigated by inserting the coin between two PS-Inductors.

Key–Words: Coin detection, Mutual inductance, Printed Spiral Inductor, Combination inductance, Self-inductance

1 Introduction

A lot of spiral shape elements are used for RFID, IC, and so on [1][2]. Especially, the spiral shapes inductors are called spiral-inductor. The spiral inductor which is generated in an IC is often used [3]. The spiral inductor is not only constructed on the chip but also on a printed board. The spiral inductors on the printed board have been easily used as a mutual inductor because the iron core does not need. That is, the mutual inductance can be easily achieved.

In this paper, we propose a novel coin detection system using the mutual inductance changes of coupled printed spiral inductors (PS-Inductors). Since the elemental composition of each coin in the world is unique, the influence of the electro magnetic field generated by two PS-Inductors, strongly depends on the coin type. In other words, the coin can be identified by investigating the mutual inductance changes of two PS-Inductors. The advantage of the proposed method is that this method is better realizable than the conventional coin detection system using the natural frequency of coin that requires the Fourier transform for detection [4]. Moreover, it can be said that the PS-Inductor generated by semicircular wiring pattern in the printed board is fit for the physical characteristic of coins.

The experimental results of various coins suggest that the proposed method can identify coins correctly.

This paper is organized as follows. In Section 2, the evaluation of the inductance of the PS-Inductor is described. The self inductance L is measured and calculated. In Section 3, the coin identification system is proposed. The coin can be distinguished by using the mutual inductance change effected by it. Section 4 shows the experimental methods and results using two coupled PS-Inductors. The coin identification is experimented using two types of PS-Inductors which have different diameter. Finally, in Section 5 the conclusion of this paper are drawn.

2 Printed Spiral Inductor

The PS-Inductor is designed by combining hemicycles. In general, a spiral inductor in an IC is composed of a square wiring pattern that is combination of straight lines.

The circle wiring pattern can provide the high Q value [5]. Therefore, PS-Inductor with circle wiring pattern is decided in this paper. Besides, its physical form suits to form of coins very well. The layout and inductance of PS-Inductor are decided by five parameters as shown in Fig. 1 and Table 1. Also, two types of PS-Inductor α and β are used in this research (see Fig. 2). The PS-Inductors are created by combining semicircular patterns by using cutting machine (see Fig. 3). The length of the conductor shortens toward the center because the conductor rolls the hemicycle from the maximum radius to the center.

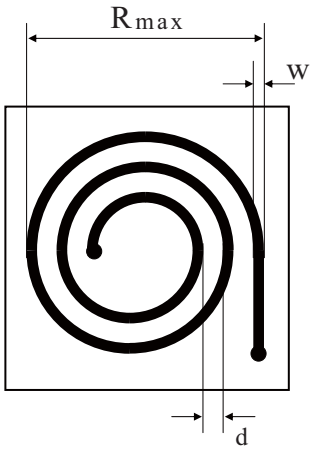

Figure 1: Design of PS-Inductor.

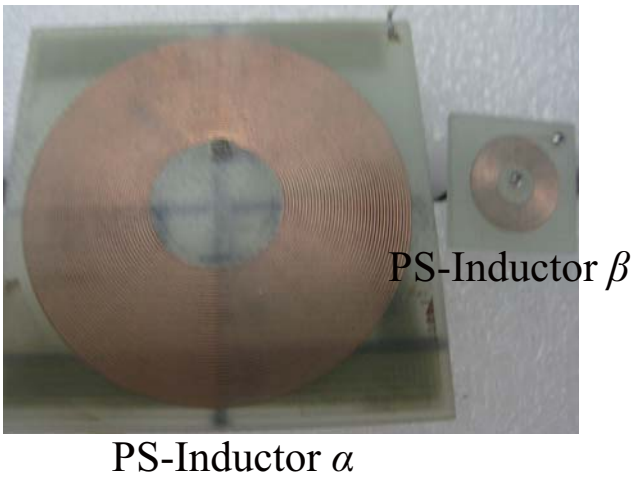

Figure 2: Picture of PS-Inductor α and PS-Inductor β

Table 1: Parameters of two kinds of PS-Inductor

	α	β
Greatest diameter R_{max}	36[mm]	10[mm]
Pattern distance d	0.2[mm]	0.11[mm]
Pattern width w	0.1[mm]	0.09[mm]
Number of harf-turn TR	80[half-turn]	30[half-turn]
Pattern thickness (single-sided)	35[um]	35[um]
Pattern thickness (double-sided)	9[um]	9[um]
Board material	Glass epoxy	Glass epoxy

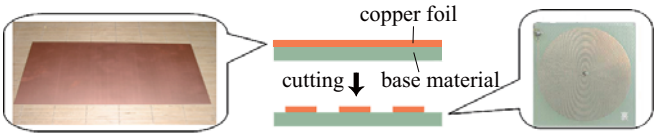

Figure 3: Fabrication of PS-Inductor

2.1 Measurement of self-inductance of the PS-Inductor

There are many methods of the measurement inductance. In this research, the inductance is measured by oscillating system which is built by combining arbitrary capacitors to a PS-Inductor. When the LC oscillation is caused, an inductance is obtained from an oscillation frequency and the capacitances. The oscillation frequency can be changed by changing values of capacitors. Therefore, the inductance of PS-Inductor can be determined by some experiments.

2.1.1 Experimental measurement of self-inductance

An inductance of high accuracy can not be obtained without an oscillation frequency and capacitances of high accuracy. Therefore, when the inductance is measured, a parasitic impedance must be considered by all possible means in the experiment circuit and the calculation obataining the inductance. The Colpitts oscillator which uses only one bipolar transistor is used because the influences of the parasitic impedances are reduced easily. Only a digital oscilloscope is used for the frequency measurements and waveform observations. Therefore, a circuit model with the measurement instrument can be drawn as like Fig. 4. An equivalent circuit of measuring impedance (see Table 2) is shown in the frame of Fig. 4. If oscillation waveform is sinusoidal shape, an inductance can be obtained from some capacitors, some resistors, an inductors, and an oscillation frequency by using following equations.

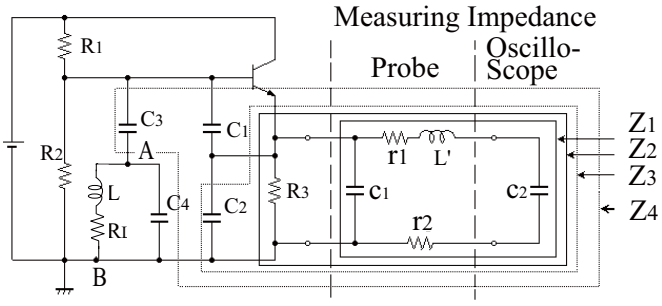

Figure 4: The circuit model with equivalent circuit of measurement equipments.

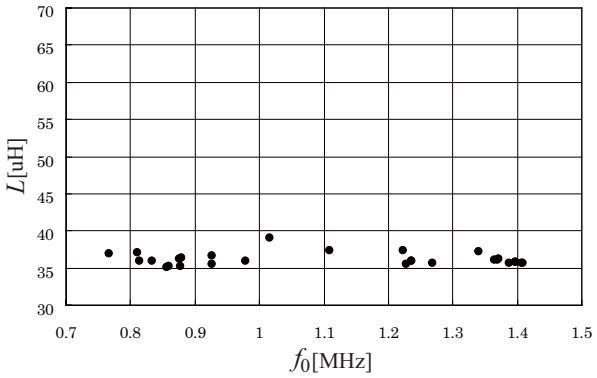

Figure 5: The inductance L vs oscillating frequency f_0 using PS-Inductor α

$$L = \frac{1 + \sqrt{1 - 4\eta^2 R^2}}{2\omega\eta}, \tag{1}$$

where

$$\eta = \omega C_4 - \frac{\zeta}{\varepsilon^2 + \zeta^2},$$
$$\varepsilon = \frac{\alpha R_3 + \omega^2 \beta\delta}{\alpha^2 + \omega^2\beta^2},$$
$$\zeta = -\frac{1}{\omega}(\frac{1}{C_1} + \frac{1}{C_3}) + \frac{\omega(\alpha\delta - \beta\gamma)}{\alpha^2 + \omega^2\beta^2}$$
$$\alpha = 1 - \omega^2(r_1 + r_2)R_3 c_2(c_1 + C_2) - \omega^2 c_2 L',$$
$$\beta = R_3(c_1 + c_2 + C_2) + c_2(r_1 + r_2) - \omega^2 L' R_3 c_2(c_1 + C_2),$$
$$\gamma = R_3 - \omega^2 c_2 R_3 L' \ , \quad \delta = (r_1 + r_2)c_2 R_3 \ ,$$

The Eq. (1) can be obtained by following equations and the oscillation condition.

$$Z_1 = \frac{1}{j\omega c_1 + \frac{1}{r_1 + j\omega L' + r_2 + \frac{1}{j\omega c_2}}},$$
$$Z_2 = \frac{1}{\frac{1}{R_3} + \frac{1}{Z_1}},$$
$$Z_3 = \frac{1}{\frac{1}{Z_2} + j\omega C_2} = \frac{\gamma + j\omega\delta}{\alpha + j\omega\beta}, \tag{2}$$
$$Z_4 = \frac{1}{j\omega C_1} + \frac{1}{j\omega C_3} + \frac{1}{Z_3} = \varepsilon + j\zeta$$
$$Y = \frac{R - j\omega L}{R^2 + \omega^2 L^2} + j\omega C_4 + \frac{1}{Z_4}$$
$$Im\{Y\} = 0.$$

The Y expresses an admittance of whole circuit. The oscillation frequency f_0 is measured while changing the capacitors C_1, C_2, C_3, and C_4. Figure 5 shows the results using Eqs. (1) and (2). The inductance L is approached to the constant value. Therefore, the inductance using Eqs. (1) and (2) is assumed as the measurement value in this research.

Table 2: The value of parasitic element (1) model number

	(1)	impedance
oscilloscope	SS-7804	C_2 = 25[pF]
	454/L/VL	C_2 = 16[pF]
	DS-9242A	R = 1[MΩ]
probe	SS-0110	C_1 =170[pF] $r_1 + r_2$ =166.73[Ω] L' =140[uH]
	SS-101R	C_1 =12[pF] $r_1 + r_2$ =9.002738[MΩ] L' =140[uH]
	PP002i	C_1 = 15.5[pF] $r_1 + r_2$ =9.05[MΩ] L' =140[uH]
transistor	2SC4083	0.8[pF]

Table 3: The Inductance of PS-Inductor

Parameter of PS-Inductor	Actual measurement	Calculated value	error [%]
α	31.944[uH]	31.265[uH]	2.17
β	1.771[uH]	1.806[uH]	1.94

2.1.2 Validation of experimental measurement

An inductance is calculated as follows:

$$L = \frac{\Phi(t)}{i(t)} \tag{3}$$

In our previous study, we developed a simulator which calculates the magnetic flux by using Biot-Savart Law and finite element method, and calculates an inductance of a PS-Inductor [6]. In this method, magnetic flux at an arbitrary domain "AT" of spacing is calculated from an arbitrary domain "SC" of conductor of the PS-Inductor below sequences.

1. Magnetic flux density of a point "a" included domain AT, and magnetic flux density of a point "b"

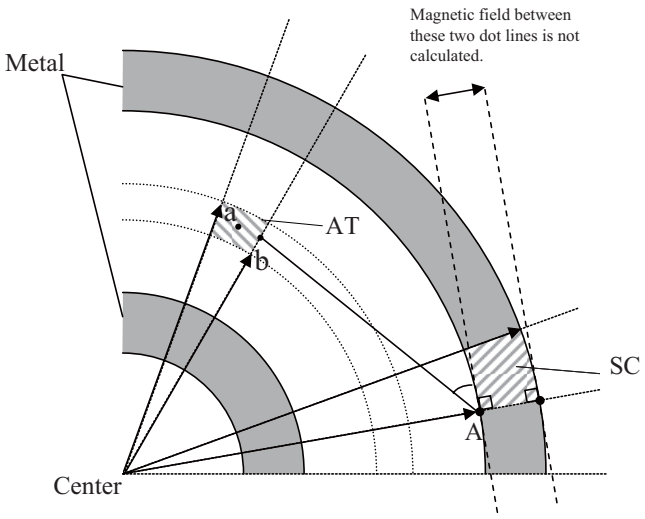

Figure 6: Analysis of inside

included domain AT are calculated from a point "A" included domain SC by using Biot-Savart Law (see Fig. 6).

2. An average of these magnetic flux densities is calculated.

3. The magnetic flux of AT is calculated by multiplying the average by a square measure of AT.

The magnetic flux of AT is obtained by applying for whole conductor, and an inductance of the PS-Inductor is calculated by applying for whole spacing. In this method, the averages of magnetic flux are calculated, because computation time becomes short and accuracy becomes good. The calculated values of self-inductances of PS-Inductor α and β are shown in Table 3.

3 Coin Identification System

The proposed coin detection system is shown in Fig. 7. The PS-Inductor is lapped over other PS-Inductor in same direction of the rotation (see Fig. 8), and the coin is passed between coupled PS-Inductors. In the proposed system, coins are detected by changes of mutual inductance of coupled PS-Inductors because each coin in the world is made from various materials and the sizes. Therefore, investigating the characteristics of the PS-Inductor is very important task.

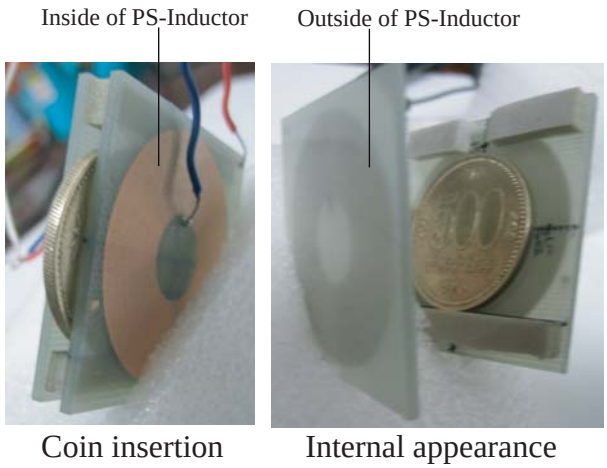

Figure 7: Proposed coin detection system

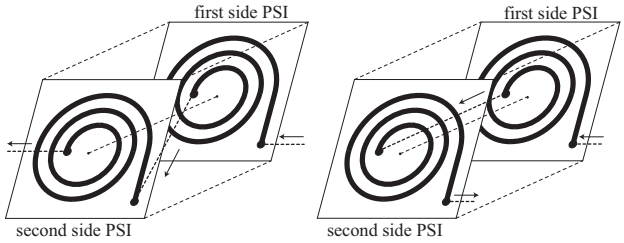

(a) Forward direction (b) Inverse direction

Figure 8: How to overlap two PS-Inductors

3.1 Measurement of mutual inductance between two PS-Inductors

3.1.1 Experimental measurement

The mutual inductance can be measured as follows.

1. The PS-Inductor is lapped over other PS-Inductor (see Fig. 8).

2. Two PS-Inductors are connected and a combination inductor L_{com} is created. There are two kinds of L_{com} by difference of connecting method (see Figs. 8, and 9). An inside terminal of the first PS-Inductor is coupled with an outside terminal of the second PS-Inductor (see Fig. 8(a)), and a L_{com} of forward direction is constructed (see Fig. 9(a)). The inside terminal of the first PS-Inductor is coupled with an inside terminal of the second PS-Inductor (see Fig. 8(b)), and a L_{com} of inverse direction is constructed (see Fig. 9(b)). The combination inductance L_{com} of forward direction is

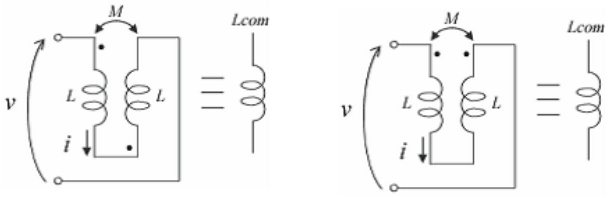

(a) Forward direction (b) Inverse direction

Figure 9: Combination inductance circuit

given by

$$\begin{aligned} v &= L_1\frac{di}{dt} + M\frac{di}{dt} + L_2\frac{di}{dt} + M\frac{di}{dt} \\ &= (L_1 + L_2 + 2M)\frac{di}{dt}, \\ L_{com} &= L_1 + L_2 + 2M, \end{aligned} \tag{4}$$

and the combination inductance L_{com} of inverse direction is obtained by

$$\begin{aligned} v &= L_1\frac{di}{dt} - M\frac{di}{dt} + L_2\frac{di}{dt} - M\frac{di}{dt} \\ &= (L_1 + L_2 - 2M)\frac{di}{dt}, \\ L_{com} &= L_1 + L_2 - 2M. \end{aligned} \tag{5}$$

Therefore, the mutual inductance M is described by

$$M = \frac{|L_{com} - L_1 - L_2|}{2}. \tag{6}$$

This proposed system uses the L_{com} of forward direction, because the L_{com} of forward direction is larger than that of inverse direction, and measurement of forward direction is easier than that of inverse direction. Therefore, we focus on only L_{com} of the forward direction.

3. The measurement circuit uses the Colpitts-oscillator shown in Fig. 10. The distance between the first PS-Inductor and the second PS-Inductor is expressed as "d". The thickness of PS-Inductor's base is expressed as "t" and t=0.0015[m]. A Collpitts-oscillator is constructed using the L_{com}. Two terminals of the L_{com} are connected with a terminal "A", and a terminal "B". The combination inductance is measured by the oscillation method using a Colpitts-oscillator. From Eq. (1), the combination inductance is calculated as

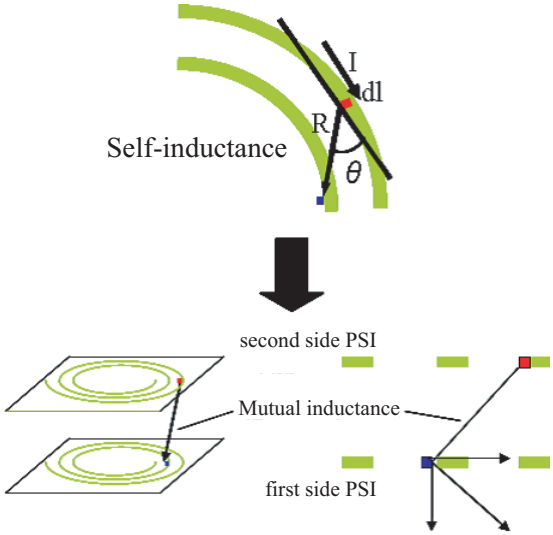

Figure 11: Three dimensional calculation

$$L_{com} = \frac{1 + \sqrt{1 - 4\eta^2 {R_{Lcom}}^2}}{2\omega\eta}, \tag{7}$$

where the R_{Lcom} expresses a resistance including in the L_{com}.

3.1.2 Theoretical approach

In [7], Nukushida et.al. proposed a new method for theoretical calculation of the mutual inductance by using the Biot-Savart law and finite element method. The calculation method is changed to three dimensional calculation from previous simulator which is composed of two dimensional calculation (see Fig. 11). The new simulator obtains the sum of a self inductance and a mutual inductance ($L + M$). The mutual inductance is calculated by subtracting self inductance L that is obtained by previous method.

3.1.3 Validation checking of experimental measurement

We experiment using two coupled PS-Inductors (see Table 1) and Colpitts-oscillator circuit (see Fig. 10). The distance d of coupled PS-Inductors α is changed into 0.0025, 0.0035, 0.0045, 0.0055 and 0.0065 [m] and coupled PS-Inductors β is changed into 0.002, 0.003, 0.004, 0.005 ,0.006 and 0.007 [m]. The mutual inductance M and combination inductance L_{com} are measured in each distance. Then we compare actual measurement results with theoretical calculation results (see Figs. 12 and 13, and Tables 4, 5, 6 and 7).

The relative error margin [%] of the combination inductance L_{com} is smaller than that of the mutual in-

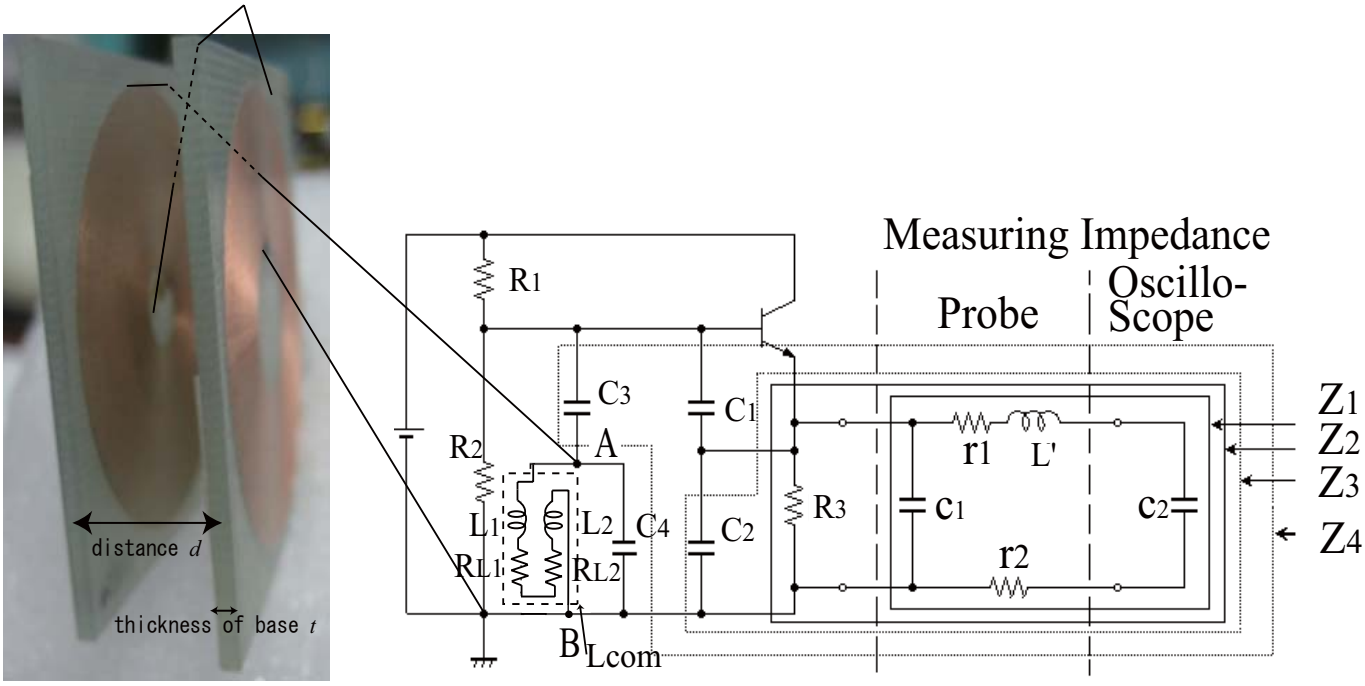

Figure 10: Coupled PS-Inductors and Colpitts-oscillator circuit

Table 4: Error of the Combination inductance L_{com} using PS-Inductor α (1)experimental measurement L_{com}[μH] (2)theoretical calculation L_{cal}[μH]

distance d[m]	(1)	(2)	error
0.0025	114.8	112.7	2.1
0.0035	109.8	107.3	2.5
0.0045	106.2	106.0	0.2
0.0055	100.5	98.53	1.97
0.0065	99.23	93.34	5.89

Table 5: Error of the Mutual inductance M of PS-Inductor α (1)experimental measurement M_{mea}[μH] (2)theoretical calculation M_{cal}[μH]

distance d[m]	(1)	(2)	error
0.0025	22.21	22.77	0.56
0.0035	19.71	20.07	0.36
0.0045	17.92	19.40	1.48
0.0055	15.06	15.68	0.62
0.0065	14.44	13.09	1.35

ductance M. In the PS-Inductor β, a large margin of error [%] especially appears to the mutual inductance. As the reason, the mutual inductance of PS-Inductor β is small. Therefore, this system should be made in the range of which distance d is small.

4 Experiments

In order to evaluate the coin identification performance, we apply our system to 10 coins (see Fig. 14, and Table 8); JPY (500, 100, 50, 10, 5 and 1) and USD (quarter, dime, nickel and penny).

Firstly, the PS-Inductor α is used. The measurement conditions are set as follows. As shown in Figs. 15, $x-y$ coordinates are fixed to the second side PS-Inductor. These coordinate are decided based on the side of the 500-yen coin, because the 500-yen coin has the largest radius in ten kinds of coins. The R_{max}, x_{max} and d are fixed as 0.018 [m], 0.03125 [m], and 0.0045 [m] respectively, because the radius of 500-yen coin is 0.01325 [m]. The center of the 500-yen coin runs throw the origin coordinate of x-axis and y-axis. In Fig. 10, the resistances R_1, R_2, and R_3 are fixed as 10 [kΩ], 10 [kΩ], and 3.3 [kΩ] respectively. The capacitors C_1, C_2, C_3, and C_4 are changed as shown in Table 9 and measured at each parameter. Measurement values are assumed an average of three values. The x expressing the position of coin is changed to -0.03125, -0.018, -0.012, -0.009, -0.006, -0.003, 0, 0.003, 0.006, 0.009, 0.012, 0.018, and 0.03125 [m], and mutual in-

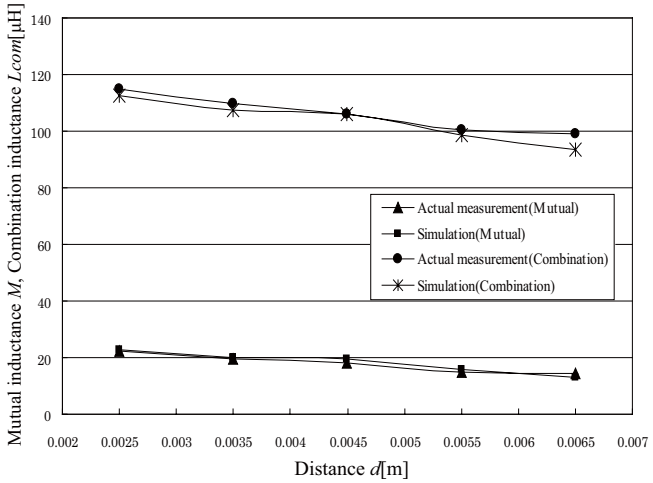

Figure 12: Distance d v.s. Mutual inductance M and Combination inductance L_{com} using PS-Inductor α

ductance and combination inductance are measured at each position of the 500-yen coin. As a result of Fig. 16, mutual inductance and combination inductance have a minimum value around x=0. For this reason, the x is changed to 0, 0.003, 0.006, 0.012, 0.018, and 0.03125[m] (see Fig. 17), and mutual inductance is measured at each position by ten coins. Fig. 18 shows changing of mutual inductances by changed of position of each coin. Therefore, the coin can be predicted by this result. Especially, many kind of the coin can be easily predicted around x=0.

Next, we use the PS-Inductor β. When the diameter of PS-Inductor is smaller than the average diameter of coins, we try constructing coin detection system. Some measurement conditions are changed from above conditions as follows. The distance d is fixed as 0.003 [m] and 0.005 [m]. In Fig. 10, the capacitors C_1, C_2, C_3, and C_4 are changed as shown

Table 6: Error of the Combination inductance L_{com} using PS-Inductor β (1)experimental measurement L_{com}[μH] (2)theoretical calculation L_{cal}[μH]

distance d[m]	(1)	(2)	error
0.002	4.33	5.28	0.95
0.003	4.23	4.94	0.71
0.004	4.00	4.73	0.73
0.005	3.92	4.60	0.68
0.006	3.81	4.51	0.7
0.007	3.70	4.45	0.75

Table 7: Error of the Mutual inductance M of PS-Inductor β (1)experimental measurement M_{mea}[μH] (2)theoretical calculation M_{cal}[μH]

distance d[m]	(1)	(2)	error
0.002	0.3955	0.4616	0.0661
0.003	0.3459	0.2933	0.0526
0.004	0.2276	0.1888	0.0388
0.005	0.1893	0.1224	0.0669
0.006	0.1323	0.0791	0.0532
0.007	0.0788	0.0501	0.0287

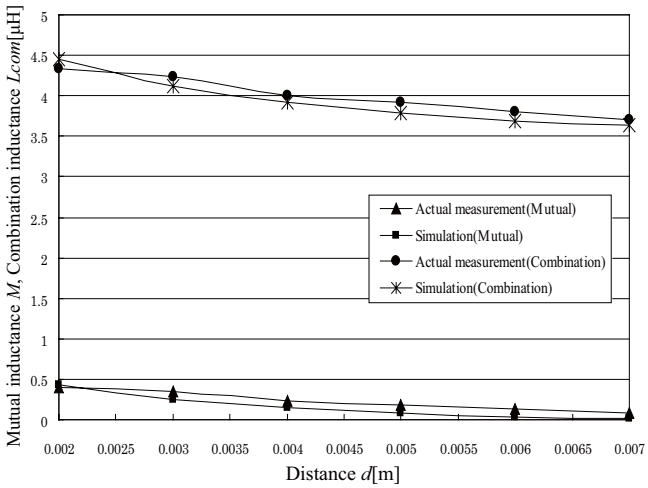

Figure 13: Distance d v.s. Mutual inductance M and Combination inductance L_{com} using PS-Inductor β

in Table 10 and measured at each value. Measurement values are assumed an average of four values. Other conditions are not changed from above conditions. Figure 19 and 20 show the results. The coin can be predicted only $d \leq 0.003$ [m]. However, from the view point obtained by Fig.20, it is difficult to identify the coins. Because the diameter of the PS-Inductor is small, the mutual inductance is small.

The coin can be predicted by the PS-Inductor especially around x=0. Furthermore, in other words, a position, a velocity, and a direction of the coin can be predicted by these results, if a kind of the coin is known, and when the coin is running through between PS-Inductors.

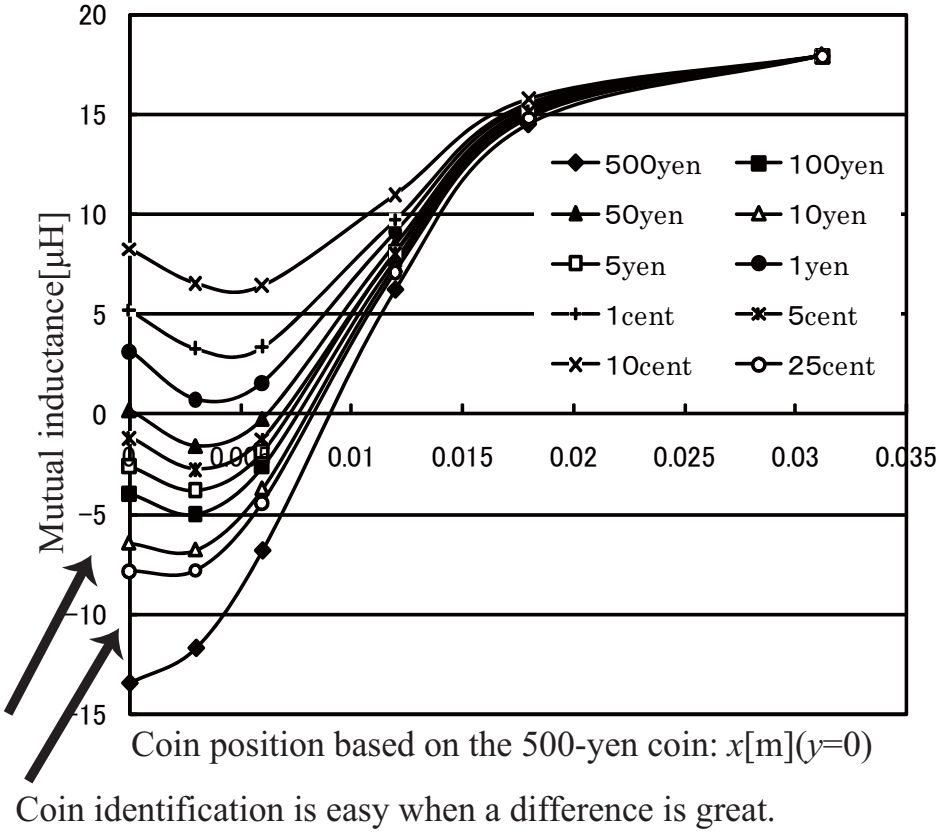

Figure 18: Coins identification of mutual inductance using PS-Inductor α

Figure 14: 10coins (JPY (500, 100, 50, 10, 5, 1) and USD (penny, nickel, dime, quarter))

5 Conclusion

In this paper, we proposed a novel coin detection system using coupled PS-Inductors. The experimental results were shown that our method can identify the 10 coins correctly. This method can identify the coins in very simple way that transition of mutual inductance between PS-Inductors by inserting the coin is only investigated. The coin identification was possible even by the PS-Inductor that is smaller than the coin. However, prediction of the kind of coin became easy by using the PS-Inductor of diameter that is larger than diameters of coins. Moreover, prediction of the kind

Table 8: Details of coin (1)outside diameter[mm] (2)thickness[mm]

coin	(1)	(2)	material
500yen	26.5	2.0	72[%]Cu, 20[%]Zn, 8[%]Ni
100yen	22.6	1.7	75[%]Cu, 25[%]Ni
50yen	21	1.5	75[%]Cu, 25[%]Ni
10yen	23.5	1.3	95[%]Cu, 3-4[%]Zn, 1-2[%]Sn
5yen	22	1.5	60-70[%]Cu, 30-40[%]Zn
1yen	20	1.54	100[%]Al
1cent	19.05	1.55	97.5[%]Zn, 2.5[%]Cu
5cent	21.21	1.95	75[%]Cu, 25[%]Ni
10cent	17.91	1.35	91.67[%]Cu, 8.33[%]Ni
25cent	24.26	1.75	91.66[%]Cu, 8.34[%]Ni

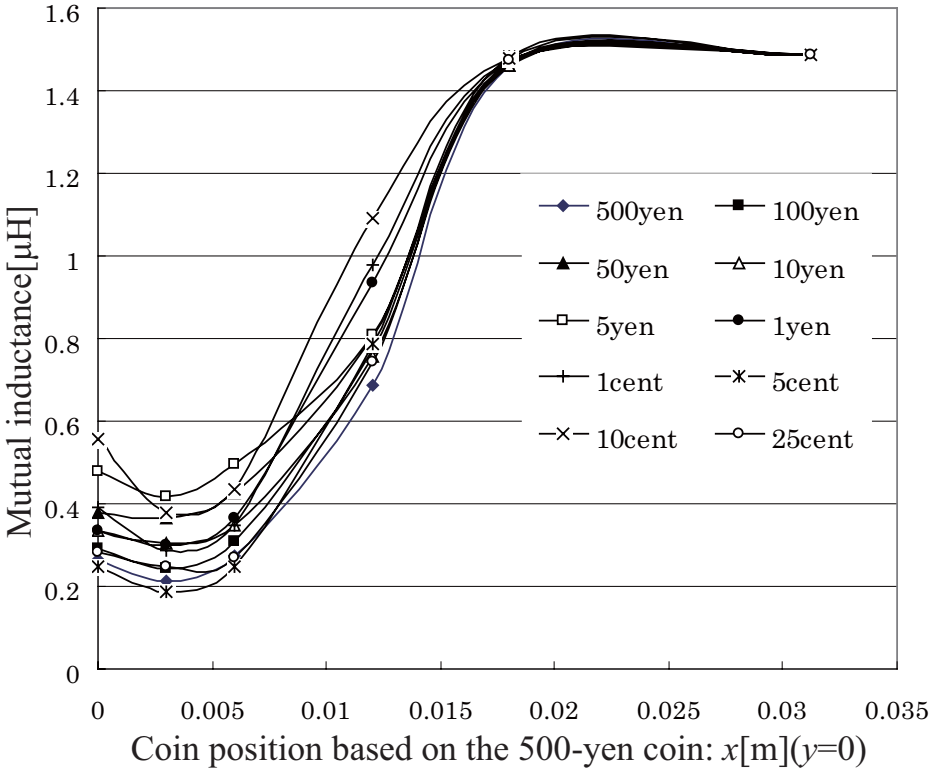

Figure 19: Coins identification of mutual inductance using PS-Inductor β d=0.003

Table 9: Combination of capacitors using parameter α (1)Combination

(1)	C_1[pF]	C_2[pF]	C_3[pF]	C_4[pF]
(γ)	4700	200	4700	100
(δ)	4700	200	9400	100
(ϵ)	6920	200	9400	100

Table 10: Combination of capacitors using parameter β (1)Combination

(1)	C_1[pF]	C_2[pF]	C_3[pF]	C_4[pF]
(ζ)	100	20	20	1
(η)	100	20	20	2
(θ)	470	20	20	2
(ι)	470	20	20	6

of coin became clear when the distance d between two PS-Inductor is short.

It can be said that a very small coin identification system at the stamp level can be constructed.

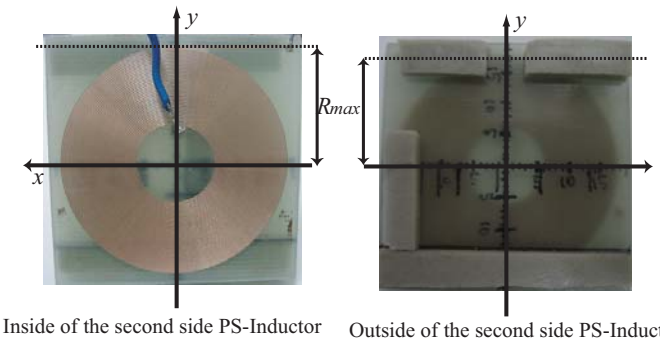

Figure 15: $x - y$ coordinates

Acknowledgment

This research is supported by the fund of the Open Research Center Project from MEXT of the Japanese Government (2007-2011). This research is supported by the Grants-in-Aid for Young Scientific Research(B) (No. 19760270) from the Japan Society for the Promotion of Science.

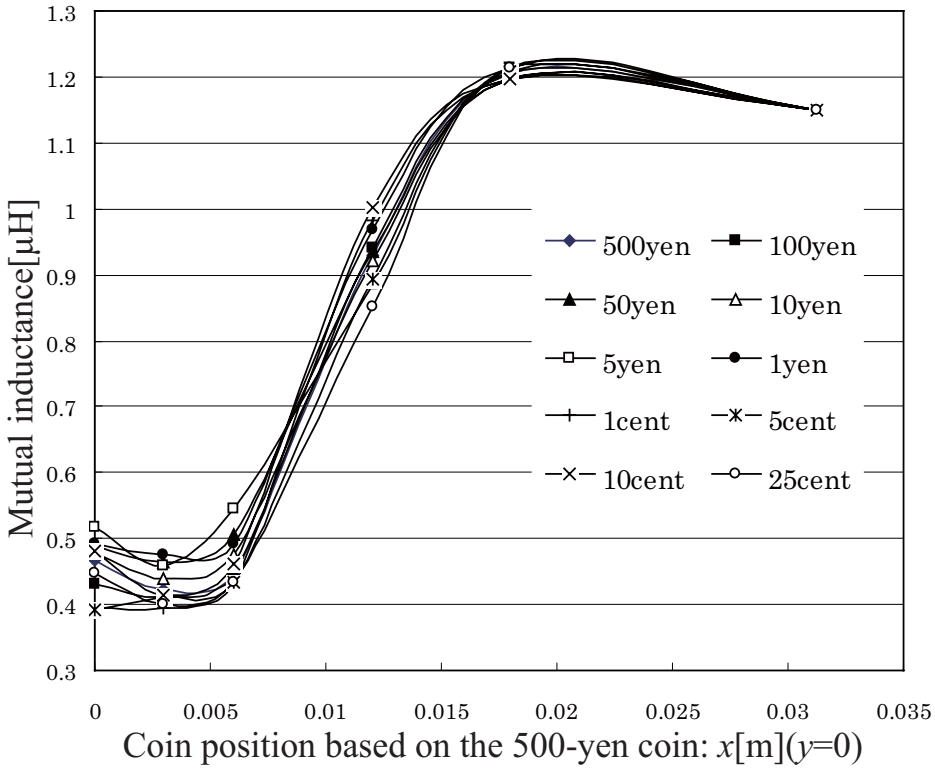

Figure 20: Coins identification of mutual inductance using PS-Inductor β d=0.005

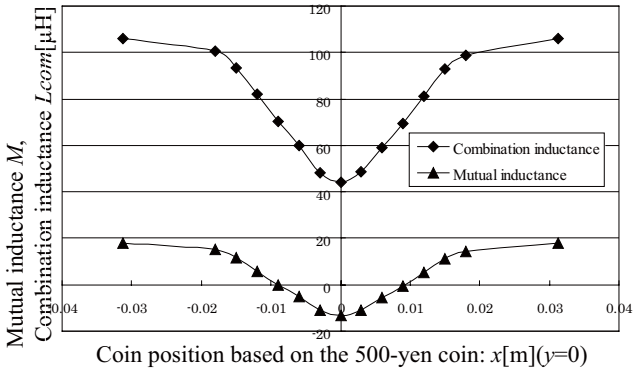

Figure 16: Characteristic by the 500-yen coin

References:

[1] J. Park, Y. Park, Y. Kim, S. Jun, "A Resistance Deviation-to-Time Interval Converter and its Application to a Passive RFID Tag for Security," World Scientific and Engineering Academy and Society(WSEAS) Circuits, Theory, and Applications, Vol.1, pp.126-130, July 2007.

[2] A. Kabir, K. C. Huang, R. Wu, P. Rapajic, "Next Generation Identity Card: RFID-based Automatic Access Control System for Universities," World Scientific and Engineering Academy and Society(WSEAS) Selected Topics on Circuits, Systems, Electronics, Control and Signal processing, pp.480-483, December 2007.

[3] K. Okada, "Design Optimization Methodology for On-Chip Spiral Inductors," IEICE Trans. Electron., Vol.E87-C, no.6, June, 2004.

[4] M. Suzuki, "Development of a simple and non-destructive examination for counterfeit coins using acoustic characteristics," Forensic Science International, Vol.177, Issue 1, pp.e5-e8, May 2008.

[5] S. S. Mohan, "Simple Accurate Expressions for Planar Spiral Inductances," IEEE Journal of solid-state circuits., Vol.37, no.10, October, 1999.

[6] M. Motoyoshi, Y. Tanaka, M. Yamauchi and M. Tanaka, "Measurement and Numeric Calculationfor Printed Spiral Inductors," Proc. of Nonlinear Theory and its Applications 2005, pp.290-293, 2005.

[7] M. Nukushina, T. Kunihiro, T. Nanko, M. Yamauchi and M. Tanaka, "Synchronization Phenomena of Coupled Colpitts Oscillators using Printed Spiral Inductors," Proc. of Nonlinear

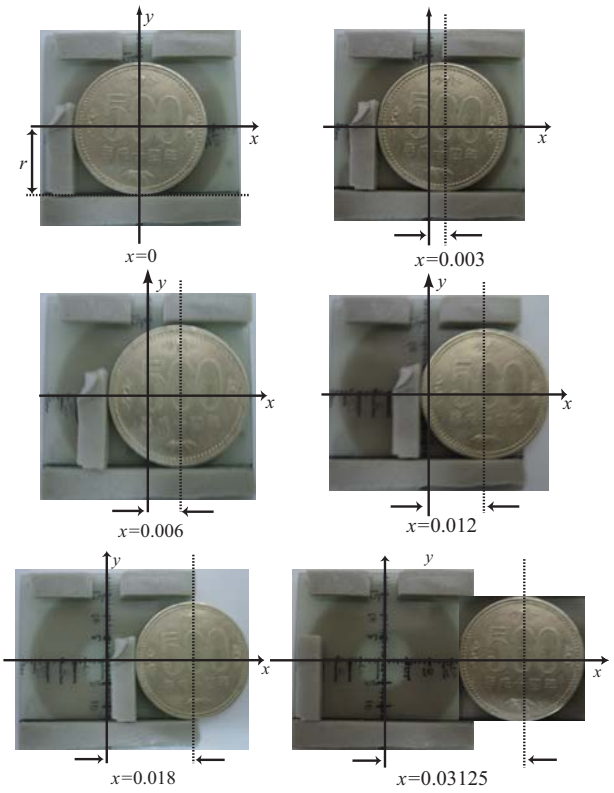

Figure 17: Setting of coordinates based on the 500-yen coin

Theory and its Applications 2007, pp.325-328, 2007.

[8] J. Fukatani, S. Yamaguchi, M. Yamauchi, H. Aomori and M. Tanaka, "A Coin Detection System by Coupled Printed Spiral Inductors"", World Scientific and Engineering Academy and Society(WSEAS) New aspects of circuits, pp.91-95, July 2008

[9] H.G. Dill, "Designing Inductors for Thin Film Applications," Electronic Design, pp.52-59, 1964.

[10] S. Y. Y. Leung and D.C.C. Lam, "Performance of Printed Polymer-Based RFID Antenna on Curvilinear Surface," IEEE CPMT Transactions in Electronic Packaging Manufacturing, Vol.30, no.3, pp.200-205, July 2007.

[11] F. J. Schmuckle, "The method of lines for the analysis of rectangular spiral inductors [in MMICs]," Microwave Theory and Techniques, IEEE Transactions on , Vol.41 , Issue6, pp.1183-118y6, June-July 1993.

[12] M. H. Chiou, "A new wideband modeling technique for spiral inductors," Semiconductor Device Research Symposium, 2003 International, pp.290-291, December 2003.

[13] R. D. Lutz, "Modeling of spiral inductors on lossy substrates for RFIC applications," Radio Frequency Integrated Circuits (RFIC) Symposium, 1998 IEEE, pp.313-316, 7-9 June 1998.